Research Square

Preprints are preliminary reports that have not undergone peer review.
They should not be considered conclusive, used to inform clinical practice,
or referenced by the media as validated information.

Simulation of CdTe, CIGS and CZTS Solar Cells using WxAMPS Software

Galib Hashmi (galib_90@yahoo.com)
Institute of Science and Technology, Bangladesh https://orcid.org/0000-0003-2047-8354
Md. Shawkot Hossain
Institute of Science and Technology, Bangladesh
Mohammad Junaebur Rashid
Dhaka University

Research Article

Keywords: Thin Film Solar Cell (TFSC), Simulation, WxAMPS Software, Buffer Layer, Absorber Layer

Posted Date: August 4th, 2021

DOI: https://doi.org/10.21203/rs.3.rs-597980/v1

License: This work is licensed under a Creative Commons Attribution 4.0 International License. Read Full License

Abstract

Solar cells made of Cadmium telluride (CdTe), copper indium gallium selenide (CIGS) and copper zinc tin sulfide (CZTS) are currently the most widely studied thin film technologies.To increase the performance and for better understanding of the behavior of CdTe, CIGS and CZTS solar cell simulations have been performed using WxAMPS software. Moreover, all the solar cells have been simulated with different buffer layers and transparent conductive oxide (TCO) layers such as Cadmium Sulphide (CdS), Zinc Sulphide (ZnS), Aluminum Zinc Oxide (AZO) and Indium Tin Oxide (ITO).Variations in the thickness and doping concentrations of TCO layers, buffer layers, and absorber layers have been done to test the performance of the solar cells.The effects of using a Back-Surface Reflector (BSR) layer made of Zinc Telluride (ZnTe) have also been studied.Furthermore, the simulation work is exceptional in this regard since all of the layers of CdTe, CIGS, and CZTS solar cells were modeled using optical parameters (absorption coefficients) from the literature. All the solar cell's open circuit voltage (Voc), short circuit current (Isc), maximum power (Pm), fill factor (FF), and photovoltaic efficiencies have been represented in this work. The simulation results may provide valuable insight in developing and better understanding of high-efficiency thin film solar cells.

1. Introduction

The fast upsurge of the global energy demand, rise of fossil fuel price, increase of global pollution, global climate changes along with the requirement of reduction of CO_2 emission from earth's atmosphere pointed out the need of sustainable renewable energy supply. Solar PV generation is a sustainable renewable energy source and currently it represents the second-largest absolute generation growth of all renewable technologies, slightly behind wind and ahead of hydropower. In 2019, worldwide solar PV panels market size was valued at 115.2 billion dollar and is anticipated to grow at a compound annual growth rate of 4.3% from 2020 to 2027. Among all types of solar PV panels the market share of thin film solar PV panels are around 40.0% in 2019. In the early 2018, the US government has imposed tariffs on imported silicon solar cells and modules. This step taken by US government may provide opportunities for thin film manufacturers [1–6].

The most leading research on thin film technology of today are copper indium gallium selenide (CIGS), Cadmium telluride (CdTe) and copper zinc tin sulfide (CZTS) solar cells. The recorded laboratory efficiency in thin film technology for CIGS, CdTe and CZTS solar cells are 23.35%, 21.0% and 10.0% respectively [7]. Since Shockley–Queisser limit has not been reached yet there is still room for improvement for these solar cells. The efficiency of solar cell is depended on number of parameters such as thickness, doping concentration, material used in the layers, front contact, back contact, deposition technique etc. The process to change any of this parameters are very hard, complex and expensive. Moreover, proper laboratory and equipments are another important aspect in solar cell designing. So, to avoid these drawbacks, simulation plays a vital role in solar cell designing. Simulation also assists the researchers to study, observe the behaviors and provides insightful knowledge about of how the devices operate. Thus, the thickness, doping concentrations and materials used in the layers have been changed in the simulation for better understanding and to obtain optimum efficiency for CIGS, CdTe and CZTS solar cells.

In the CdTe solar cell simulation study, Tinedert et al. used Silvaco-Atlas simulation software to design and simulate a CdTe solar cell and obtained 23% efficiency using CdS 0.1 μm thick CdS layer [8]. Nykyruy et al. simulated a 17.15% CdS/CdTe heterojunction solar cell using the SCAPS-1D software [9]. Using a different simulation software called wxAMPS, Devanshi Parashar et al. simulated a 17.66% efficient ZnO/CdS/CdTe solar cell by optimization of the thickness of the layers [10]. Shoewu et al., Fardi et al. and many more have done research on CdTe solar cell and experimental and numerical investigations are still going on [11–12]. In the CIGS solar cell simulation study, Rihana et al. used SnO_2:F (Fluorine doped Tin Oxide) as window layer in SCAPS-1D software and simulated a CIGS based thin film solar cell with 13.85% efficiency [13]. By means of the same software, H. Heriche et al. conducted simulation on ZnO/CdS/CIGS and ZnO/CdS/CIGS/Si solar cells. The efficiencies of the solar cells were 16.39% and 21.3% respectively [14]. Silvaco-Atlas simulation software has been used by Elbar et al. to simulate two different ZnO/CdS/CIGS solar cells and achieved efficiencies 18.92% and 20.32% respectively through the optimization of the thickness of the layers [15]. In reference [16–19], there are reports on CIGS solar cell simulation work and exploration on this study is still ongoing. In the CZTS solar cell simulation study, Jhuma et al. performed three buffer layers (CdS, ZnS, $Cd_{0.4}Zn_{0.6}S$) optimization by SCAPS-1D software and obtained efficiencies 11.20%, 11.47% and 11.58% respectively for the CZTS solar cells [20/?]. In addition, F. Belarbi et al. also had used SCAPS-1D software and done a comparative study with three buffer materials (CdS, SnS_2, Zn_2SnO_4) and obtained maximum efficiency of 12.73% by ZnO/SnS_2/ CZTS/ Mo/glass structure solar cell [21]. Furthermore, Abdelbaki Cherouana et al. has done simulation on CZTS solar cell with silicon back surface field using SCAPS-1D software and attained 10.69% efficiency [22]. Recent studies mentioned in the reference [23–25], represents that prominent research on CZTS solar cell simulation work is still continuing.

From the briefly mentioned literature review indicates that, there are many simulation softwares which are being used for solar cell design. Some of the softwares are PC-1D (Personal Computer - One Dimension), WxAMPS (Widget Provided Analysis of Microelectronic and Photonic Structures), SCAPS-1D (Solar Cell Capacitance Simulator- One Dimension), Silvaco-Atlas Technology Computer Aided Design (TCAD) software etc. In this work, WxAMPS simulation software has been used for all kinds of thin film solar cell simulation. This software has been used because optical parameters are by default not given whereas, in SCAPS software there is option to use the default optical parameters in the simulation. Moreover, it is an easy operating thin film simulation software.

The main difference between this work and others are, for all the layers of CdTe, CIGS and CZTS solar cell optical parameters (absorption coefficients) value found in the literature have been used in the WxAMPS simulation software. Moreover, simulation have been conducted with three types of absorber layers such as CdTe, CIGS and CZTS layer. Study shows Zinc Sulphide (ZnS) is a promising material and can be used as an alternative to the commonly used Cadmium Sulphide (CdS) buffer layer. Thus, these two buffer layers have been utilized for the three different types of solar cells. Among all the transparent conductive oxide (TCO) layers, indium tin oxide (ITO) and aluminum zinc oxide (AZO) are broadly used in commercial applications as they can reduce the energy loss by as much as 30% [26]. Therefore, both of these TCO layers have been used in the solar cell simulations. The performance of with and without Zinc telluride (ZnTe) Back-Surface Reflector (BSR) layers have been investigated also. Overall the thickness, doping concentrations and materials used in the

layers have been altered in the simulation for optimization of CdTe, CIGS and CZTS solar cells. All the observed results including Voc, Jsc, fill factor (FF), and efficiency (η) and performance analysis of different solar cells have been discussed in this paper.

2. Thin Film Solar Cell (Tfsc)

A solar cell (also called a photovoltaic cell, as shown in Fig. 1) is an electrical device that converts the energy of light directly into electricity by the photovoltaic effect [27]. Where, the photovoltaic effect is the process that generates voltage in a photovoltaic cell when it is exposed to light or other radiant energy [28].

A thin film solar cell is a solar cell whose thicknesses varies from few micrometers to few nanometers and it is constructed by depositing some thin layers consecutively. A general structure of thin film solar cell is depicted in Fig. 2. A thin film solar cell consists of different layers. Such as front contact / Transparent Conducting Oxide (TCO), window layer, buffer layer, absorber layer, back surface reflector (BSR), back contact and substrate. The TCO and window layer can be separate or can be the same as shown in Fig. 2 (a) and (b). Each layer has a specific function and these layers are described briefly in the following section.

Front contact is the topmost layer of the thin film solar cell. The main function of this layer is to collect the current produced by the cell and serve it to an outer circuit or load. 1st generation solar cell has opaque grid finger front contacts. Whereas, in 2nd generation solar cell (Thin Film) the front contact is designed differently. The front contact is a transparent conductive oxide (TCO) layer. The conductive oxide provides the same function as 1st generation contact and for being transparent, light can easily enter the TFSC. Thus, the front contact is also known as transparent conductive oxide (TCO) layer. The TCO being transparent, can be assumed it behaves like a window for the solar cell by which most of the light enters into the solar cell. Thus, it is also called window layer and both TCO and window layer can be the same (As shown in Fig. 2 (a)). However, when the transparency of the TCO layer increases, the resistance also increases proportionally. The resistance of TCO layer needs to be low because of the current collection from the buffer layer. To tradeoff between transparency and conductance, sometimes TCO and window layers are separated (As shown in Fig. 2 (b)) to improve the overall performance of the solar cell. The bandgap of the window layer must be high for greater light trapping and absorption of high energy photon. In this layer, a great amount of light is absorbed to the cell. Under the window layer is the buffer layer. The buffer layer in general is an N-type semiconductor material, which along with the P-type absorber layer form the P-N junction of TFSC. The buffer layer is named so like this, because it adjusts the bandgap matching between the absorber layer and the window layer. The doping concentration of a buffer layer must be high so that the number of minority carrier is reduced and as a result recombination can be minimized. Recombination on this layer degrade the working ability of the solar cell. Absorber layer absorb the low energy photon as the bandgap of this semiconductor material is low. In general the absorber layer is a P-type semiconductor material and have a higher contribution from photo-generated electron-hole (e-h) pairs [29]. Furthermore, the thickness of this layer is much higher than that of the other layers used in the solar cell. Not all of the TFSC architectures has the Back-Surface Reflector (BSR) layer. In the recent years, to improve the performance of back contact and to reduce the recombination in the structure, a back surface reflector (BSR) layer has been used. The essential role of this layer is to confine the photogenerated minority carriers and make sure is close enough to reach the P-N junction so that current could be proficiently collected [26, 30]. By using back contact layer a full path for the current carrying circuit is made and is used for the purpose of current collection from the cell. It is deposited on the substrate layer and it does make contact with the back surface reflector (BSR) layer or absorber layer. On the substrate, the consecutive layers are deposited. The substrate can be of glass, plastic etc. Soda Lime Glass (SLG) is generally used as substrate in TFSC.

2.1 Types of Thin Film Solar Cell (TFSC)

In TFSC technology, there are different types of solar cells. These solar cells are named after the material used in the absorber layer. The first type of TFSC is amorphous silicon solar cell. This type of TFSC uses bulk amount of silicon. However, to reduce the cost, the thin film technology has been evolved and many solar cells like CdTe, CIGS, CZTS etc. have been designed successively. In this research CdTe, CIGS and CZTS TFSCs have been simulated and optimized. Thus, some information of each of these cells are discussed in the following section.

2.1.1 Cadmium Telluride (CdTe) Solar Cell

Cadmium Telluride (chemical formula: CdTe) is the second most utilized solar cell technology today. The first is still 1st generation silicon solar cell. CdTe is a suitable material for solar cell operation. Because, it has a direct bandgap of 1.45 eV for AM 1.5 solar spectrum and is nearly optimal for converting sunlight into electricity [31]. Furthermore, one of the great advantage of CdTe solar cell is, it is a low cost manufacturing technology. Nonetheless, the main problem with CdTe solar cell is its toxicity. Cd is harmful for environment. By using Cadmium sulfide (CdS) as buffer layer the toxicity of CdTe solar cell is reduced as CdS material is less toxic than the Cd material alone. Currently many research is running for finding the alternative of CdS buffer layer to reduce the toxicity effect. At present, prominent research is going on the following buffer material: Zinc selenide (ZnSe), Zinc cadmium sulfide (ZnCdS), Indium sulfide (In_2S_3), Zinc sulfide (ZnS) and Indium selenide (In_2Se_3). In addition to solve the toxicity problem, research on Window / TCO layers and Back-Surface Reflectors are still going on for the improvement of the efficiency of CdTe solar cell. The popular current research materials with thickness for Window / TCO layers and Back-Surface Reflectors have been tabulated in Table 1.

2.1.2 Copper Indium Gallium Selenide (CIGS) Solar Cell

Copper Indium Gallium Selenide (CIGS) is another kind of TFSC where CIGS is used as absorber layer. The CIGS material is a solid solution of copper indium selenide (CIS) and copper gallium selenide. It has a chemical formula of $CuIn_{(1-x)}Ga_{(x)}Se_2$. Where the value of x can vary from 0 (pure copper indium selenide) to 1 (pure copper gallium selenide) The bandgap of CIGS material varying continuously with x from about 1.0 eV (for copper indium selenide) to about 1.7 eV (for copper gallium selenide). As CIGS material is used instead of CdTe as absorber layer, CIGS has advantage over CdTe in toxicity aspects. CIGS film acts as a direct bandgap semiconductor. Nevertheless, the toxic effect is still has not been completely removed as in general CdS is used as buffer layer. However, alternative materials are used as a substitute of CdS nowadays. They are zinc sulfide (ZnS), Zinc selenide (ZnSe), Indium sulfide (In_2S_3), Zinc Oxide (ZnO) and

magnesium zinc oxide (MgZnO). By varying the thickness of materials in different layers and also by utilizing different combinations of materials, research on CIGS TFSC is still continuing. Summarized thickness, materials and associated layers are given away in Table 1.

2.1.3 Copper Zinc Tin Sulfide (CZTS) Solar Cell

One of the critical issues with CdTe and CIGS based solar cells are, the less availability of tellurium and indium on earth. To solve this problem, Copper Zinc Tin Sulfide (CZTS) material has drawn the attention of the researchers as an alternative absorber layer. Furthermore, CZTS is a non-toxic, low cost, earth-abundant material having reasonable electrical and optical properties. The chemical formula of CZTS is Cu_2ZnSnS_4. CZTS also has a direct and tunable band gap (Eg ~ 1.45 eV–1.6 eV). Yet detoxification of Cd from CdS buffer layer is still an issue for its advancement. To avoid this problem, other options include using zinc sulfide (ZnS) / Zinc selenide (ZnSe) / Zinc cadmium sulfide (ZnCdS) / Indium sulfide (In_2S_3) / zinc sulfide (ZnS) or Indium selenide (In_2Se_3) as buffer layer. CZTS solar cell is comparatively new than CdTe and CIGS TFSC. Thus, research on Window / TCO layer is also underway. Parameters of associated layers and materials of CZTS solar cell are presented in Table 1.

Table 1: General List of Different TFSC with Associated Layers, Thickness & Materials

		CdTe Solar Cell	CIGS Solar Cell	CZTS Solar Cell
Layers name	**Thickness**	**Material list**	**Material list**	**Material list**
Window/TCO	(0.1 to 1.0) µm	ITO/CTO/FTO/ZnO/ SnO_2/ZnMgO/AZO	ITO/CTO/FTO/ZnO/ SnO_2/ZnMgO/AZO	ITO/CTO/FTO/ZnO/ SnO_2/ZnMgO/AZO
Buffer layer	(20-100) nm	CdS/ZnSe/ZnCdS/In_2S_3/ ZnS/In_2Se_3	CdS/ZnSe/In2S3/ ZnS/ZnO/MgZnO	CdS/ZnSe/ZnCdS/In_2S_3/ ZnS/In_2Se_3
Absorber layer	(1-6) µm	CdTe	CIGS	CZTS
BSR	(0.1-1) µm	ZnTe/Sb_2Te_3	ZnTe/Sb_2Te_3	-
Back contact	(0.5-1.0) µm	Ag/Mo/Al	Ag/Mo/Al	Ag/Mo/Al
Substrate layer	(1-2) µm	Glass/plastic	Glass/plastic	Glass/plastic

Footnote: The highlighted red coloured materials are used in the simulation.

3. Wxamps Simulation Software Operating Procedure [32]

WxAMPS (**W**idget **P**rovided **A**nalysis of **M**icroelectronic and **P**hotonic **S**tructures) is an improved version of AMPS (**A**nalysis of **M**icroelectronic and **P**hotonic **S**tructures) software. The AMPS software was developed by Stephen Fonash and his group at the Pennsylvania State University, U.S.A. and wasreleased in 1997 [33]. Then in 2012, AMPS has been improved to WxAMPS software at the University of Illinois at Urbana Champaign, in collaboration with Nankai University of China [34]. It is a popular simulation software for modeling of thin film solar cells. In WxAMPS there is no limit to the number of layers allowed.

The dimension and input power of the solar cells are considered 1cm ×1cm and 100 mW/cm^2 respectively in the sofware. The pictorial diagram of the graphical user interface is given in Fig. 3. To make the simulation software operational, the simulation procedure needs to be carried out in three steps. In the first step, the ambient operational environment is selected. Where, the standard value of room temperature 300K (25^0c) and solar spectrum air mass 1.5G is considered. For proper simulation click the light on and load the AM1_5G 1 sun.spe and Light0_0.7_1.vol bias voltage file. Secondly, the materials operational environment is selected. Here, for each layer of the TFSC, different electrical and optical properties of the materials are entered. Finally, the simulation process is executed by pressing the run button and the outputs are shown in the results section.

3.1 Physical Parameters of Different Layers:

In WxAMPS simulation software's materials operational environment (also known as the "Material" section), specified electrical parameters values of every layers must be included to make the simulation to work properly. Some of the electrical parameters are bandgap, electron affinity, hole and electron mobility. The values of the electrical parameters for some materials are stated in a Table 2.

Table 2
The physical parameters of different layers

Parameters	CdTe [35–36]	CIGS [37–40]	CZTS [20, 41]	CdS [35, 38]	ZnS [20, 38, 42]	AZO [35]	ITO [20]	ZnTe [35]
W (μ_m)	1–6	1–4	1–4	0.02–0.1	0.02–0.1	0. 1–1	0.1 -1	0.1-1
E_g (eV)	1.50	1.13	1.5	2.42	3.5	3.30	3.6	2.26
ε_r	9.4	13.6	10	10	10	9.0	10	9.67
χ_e (eV)	4.6	4.41	4.5	4.3	4.5	4.35	4.1	3.50
μ_n (cm^2/vs)	320	100	100	100/350	50	100	50	330
μ_p (cm^2/vs)	40	25	25	25/50	20	25	75	80
N_c (cm^{-3})	8×10^{17}	2.2×10^{18}	2.2×10^{18}	2.2×10^{17}	1.5×10^{18}	2.2×10^{18}	2.2×10^{18}	7×10^{16}
N_v (cm^{-3})	1.8×10^{19}	1.8×10^{19}	1.8×10^{19}	1.8×10^{18}	1.8×10^{18}	1.8×10^{19}	1.8×10^{19}	2×10^{19}
N_D (cm^{-3}) Reference Value	0	0	1×10^{1}	1×10^{17}	5×10^{15}	1×10^{18}	1×10^{19}	0
N_A (cm^{-3}) Reference Value	2×10^{16}	2×10^{16}	2×10^{14}	0	0	0	0	1×10^{18}

Footnote

Thickness - W (μ_m), Bandgap - Eg (eV), Relative Permittivity - ε_r, Electron affinity - χe (eV), Electron mobility - μ_n (cm^2/vs), Hole mobility - μ_p (cm^2/vs), Conduction band density - N_c (cm^{-3}), Valence band density - N_v (cm^{-3}), Donor concentration - N_D (cm^{-3}), Acceptor concentration - N_A (cm^{-3})

Some of the parameters can be changed but in limited versions. The thickness of the layer and doping concentrations of N-type or P-type material can be changed. By varying these parameters, an improved result can be obtained.

Alongside electrical parameters one has to input the optical values like the wavelengths and their respective absorption coefficients. Every material has different action on different wavelength. Thus, the wavelengths of different materials and associated absorption coefficients are distinct with each other. In Table 3, the absorption coefficients for all of the materials used in the simulation are listed. By giving emphasis on the visible spectrum, the wavelengths from 320–800 nm have been taken into consideration for simulation in this work. The values of absorption coefficients are compulsory, otherwise the simulation will not run. To include the absorption coefficient value click the **From AB** button in the optical tab of the “Material” section. Then nm and m-1 will appear in the lower portion. Include relevant wavelength and absorption coefficient accordingly e.g inputting the absorption coefficient value of 1.6587e + 006 alongside 400 nm wavelength. By default, a lot of wavelengths will appear after clicking the **From AB** button. So the easy process is to save the needed wavelengths and associated absorption coefficients data by clicking To XML(.absx). Then open the ABSX file with note pad and reduce the number of unnecessary wavelength slots, if necessary put additional absorption coefficients and associated wavelength values, rename the file and then load the renamed .absx data by clicking **From File** button in the optical tab of the “Material” section. From Table 1, it is seen that, materials like Ag, Cu, Mo or Al can be used as back contact. But in this work no back contact has been used in the simulation as WxAMPS simulation software does not offer any option to provide back contact. But in real life scenario, there must be a back contact for current collection from the device. Furthermore, substrate selection is also not possible in WxAMPS software. The substrate is a material where, the consecutive layers are deposited. It can be glass, plastic etc. It is recommended to use Soda Lime Glass (SLG) as substrate in thin film. Because, SLG is slightly different from normal glass. When SLG is used as a substrate the sodium ions diffuses into the absorber layer and improves the working capability of the solar cells. The simulations have been done for only front contacts, buffer layers, absorber layers and BSRs. Since there exist different materials for a single layer, a number of combinations can be possible for a single solar cell. Every combinations have different impacts on the efficiency of the solar cells. So, for examination of these impacts highest number of possible combinations have been done in simulations for CdTe, CIGS and CZTS solar cells.

Table 3
Wavelength and their respective Absorption coefficient

Wavelength (nm)	CdS [43]	CdTe [43]	ZnTe [44]	AZO [43]	CZTS [45]	ZnS [46]	CIGS [47]	ITO [48–50]
	α (m^{-1})	α (m^{-1})	α (m^{-1})	α (m^{-1})	α (m^{-1})	α (m^{-1})	α (m^{-1})	α (m^{-1})
320	1.49×10^{7}	6.94×10^{7}	6.32×10^{7}	6.06×10^{6}	-	1.17×10^{7}	4.03×10^{7}	6.66×10^{6}
360	1.26×10^{7}	4.52×10^{7}	3.70×10^{7}	4.84×10^{5}	-	1.88×10^{6}	3.51×10^{7}	2.30×10^{6}
400	1.06×10^{7}	2.22×10^{7}	1.43×10^{7}	3.62×10^{4}	5.46×10^{6}	2.51×10^{5}	3.61×10^{7}	9.0×10^{5}
440	9.05×10^{6}	1.40×10^{7}	1.01×10^{7}	2.46×10^{4}	5.38×10^{6}	8.56×10^{4}	2.72×10^{7}	3.95×10^{5}
480	7.23×10^{6}	1.17×10^{7}	7.67×10^{6}	2.61×10^{4}	5.24×10^{6}	2.61×10^{4}	1.87×10^{7}	1.99×10^{5}
520	7.12×10^{5}	9.66×10^{6}	5.20×10^{6}	3.19×10^{4}	5.19×10^{6}	-	1.41×10^{7}	1.24×10^{5}
560	5.14×10^{2}	7.86×10^{6}	2.19×10^{6}	4.00×10^{4}	5.18×10^{6}	2.24×10^{4}	1.13×10^{7}	1.02×10^{5}
600	0.007364	6.44×10^{6}	1.47×10^{6}	5.00×10^{4}	5.26×10^{6}	4.18×10^{4}	1.02×10^{7}	1.04×10^{5}
640	4.35×10^{-13}	5.38×10^{6}	1.20×10^{6}	6.19×10^{4}	5.33×10^{6}	3.92×10^{4}	8.89×10^{6}	1.19×10^{5}
680	$(-)2.54 \times 10^{-14}$	4.42×10^{6}	1.02×10^{6}	7.58×10^{4}	5.09×10^{6}	9.24×10^{4}	7.47×10^{6}	1.37×10^{5}
720	2.0×10^{-14}	3.37×10^{6}	8.82×10^{5}	9.19×10^{4}	5.21×10^{6}	1.04×10^{5}	6.71×10^{6}	1.61×10^{5}
760	3.87×10^{-25}	2.30×10^{6}	7.72×10^{5}	1.10×10^{5}	5.24×10^{6}	1.15×10^{5}	6.35×10^{6}	1.85×10^{5}
800	$(-)2.69 \times 10^{-14}$	1.30×10^{6}	6.84×10^{5}	1.31×10^{5}	5.26×10^{6}	1.41×10^{5}	5.65×10^{6}	2.12×10^{5}

The materials whose electrical and optical values are well established in the literature (as shown in Table 2 and Table 3) have been used in the simulations of the CdTe, CIGS and CZTS solar cells. The thickness range used for simulations of CIGS and CZTS solar cells are 1–4 μm and for CdTe it is 1–6 μm. Moreover, to find out the best TCO with optimum thickness, thickness variation of 0. 1–1.0 μm have been done with Aluminum-doped zinc oxide (AZO) and Indium tin oxide (ITO) for all the solar cells. Cadmium sulfide (CdS) and its alternative Zinc sulfide (ZnS) have been used as buffer layers. Their thickness have been changed form 0.01–0.1 μm in the simulation. Apart for CZTS solar cell (as simulation could not be done due to numerical failure), ZnTe with thickness of 1 μm have been used as BSR for CdTe and CIGS solar cells. For all the materials the reference values of donor and acceptor concentrations (As tabulated in Table 2) have been used at the beginning of the simulations, later those values have been changed for optimization. In this simulation work, all the combinations used for CdTe, CIGS and CZTS solar cells and their respective outcomes have been disclosed in the results and discussion section.

4. Results And Discussion

4.1 Impacts of Thickness Variation of transparent conductive oxide (TCO) layers & Back-Surface Reflector (BSR)

At first, the thickness of buffer layer, absorber layer and the BSR layer were kept at 0.02 μm, 2 μm & 1 μm respectively. Then by keeping the doping concentration of each layer constant, initially 20 different combinations of thin film solar cell has been simulated to find the best TCO. The combinations are as follows:1) AZO_CdS_CdTe_ZnTe, 2) AZO_CdS_CdTe, 3) AZO_CdS_CIGS_ZnTe, 4) AZO_CdS_CIGS, 5) AZO_CdS_CZTS, 6) AZO_ZnS_CdTe_ZnTe, 7) AZO_ZnS_CdTe, 8) AZO_ZnS_CIGS_ZnTe, 9) AZO_ZnS_CIGS, 10) AZO_ZnS_CZTS, 11) ITO_CdS_CdTe_ZnTe, 12) ITO_CdS_CdTe, 13) ITO_CdS_CIGS_ZnTe, 14) ITO_CdS_CIGS, 15) AZO_CdS_CZTS, 16) AZO_ZnS_CdTe_ZnTe, 17) ITO_ZnS_CdTe, 18) ITO_ZnS_CIGS_ZnTe, 19) ITO_ZnS_CIGS, and 20) ITO_ZnS_CZTS. Here, in the combinations at first the TCO layer is mentioned, then with an underscore the buffer layer is stated, after that the absorber layer is acknowledged and lastly the BSR layer (except CZTS solar cell) is declared. To find out the optimum thickness of the TCOs the thicknesses have been varied from 0. 1 to 1.0 μm. The thickness versus efficiency of all the 20 combinations are shown in Figs. 4 & 5.

From the simulation, it is observed that 0.1 μm thickness has the highest efficiency in all the cases of TCO. Whenever, the thickness of TCOs is increased from 0.1 to 1 μm the consequences are always associated with the reduction in the efficiency. This is due to the fact that, when the thickness is increased the sheet resistance is increased and thus the overall conductivity is decreased. From the experimental study, it is in agreement that if the sheet resistance increases, then the overall conductivity also decreases [51]. However, it is also seen from the experimental study that low thickness does not always have the best value. Because when a layer thickness is minimized a lot of complications arises and in this simulation those factors have not been taken into consideration. Also from Fig. 4 it is seen that the transparent conductive Al-doped ZnO (AZO) thin films have less variations with efficiency due to thickness variations than transparent conductive indium tin oxide (ITO). The reason is, due to the alteration of the thickness the variation in sheet resistance is low for AZO in compare to ITO, where sheet resistance changes considerably. Highest efficiency of 21.15% has being achieved by AZO_ZnS_CZTS solar cell. Closely followed by AZO_CdS_CdTe_ZnTe solar cell with 20.18% efficiency. Later in the simulation when doping concentrations have been optimized (As shown in Table 4) it is seen that, in all the cases AZO's performance is better than ITO layer. It may be due to the reason that, AZO layer has better optical transparency and thermal stability [52]. Nevertheless, the debate between the values of AZO vs. ITO for thin film solar cell is still ongoing [53]. Currently both TCO materials are used by the manufacturers.

Simulation has been carried out with ZnTe as BSR layer with 1 μm thickness. Unfortunately, numerical error has been obtained for some of the parameters for CZTS solar cell. Thus, ZnTe layer has been used for CdTe and CIGS solar cell only. It has been found that for all the combinations the efficiency of thin film solar cells with ZnTe BSR layer are more than without BSR layer. This is because the BSR layer reflects the incident light back to the absorber layer of the solar cell, thus extending the light path and causing the "light trapping effect"[54]. Reducing the thickness of ZnTe layer increases the efficiency of solar cell, but has not been done elaborately. So it is proposed as the future work of this research.

4.2 Impacts of Doping Concentrations and Thickness Variations of Buffer Layers and Absorber Layers

One of the key factors to increase the efficiency of the solar cell is to optimize the doping concentration. The doping concentration of the P-type and N-type material of 12 different combinations of TFSC have been changed in this simulation. The 12 different combinations are as follows: 1) AZO_CdS_CdTe_ZnTe, 2) AZO_CdS_CIGS_ZnTe, 3) AZO_CdS_CZTS, 4) AZO_ZnS_CdTe_ZnTe, 5) AZO_ZnS_CIGS_ZnTe, 6) AZO_ZnS_CZTS, 7) ITO_CdS_CdTe_ZnTe, 8) ITO_CdS_CIGS_ZnTe, 9) ITO_CdS_CZTS, 10) ITO_ZnS_CdTe_ZnTe, 11) ITO_ZnS_CIGS_ZnTe and 12) ITO_ZnS_CZTS. It has been shown in Sect. 4.1 that the CdTe and CIGS solar cell with ZnTe BSR layer has better performance than without any BSR layer. Thus, the 8 combinations of CdTe and CIGS solar cell without ZnTe BSR layer have been excluded in the simulation. In general, the doping concentrations of P-type & N-type material varies from 1×10^{12} cm^{-3} to 1×10^{20} cm^{-3}. Thus, the doping concentrations of buffer layers and absorber layers of CZTS solar cell and CdTe and CIGS solar cells with BSR layer have been altered in that range. In addition of changing the doping concentration, the thickness of buffer layers and absorber layers have also been varied in the simulation. The simulation regarding these results are summarized and shown in Table 4.

The highlighted blue colours in Table 4 represent the results obtained from the reference doping concentrations found in the literature. Doping concentrations of P-type and N-type layers have been increased and decreased from the reference values (blue highlighted colours) to get the optimum doping concentration values (yellow highlighted colours). But the doping concentrations of TCO and BSR have been kept constant at the reference values during the simulation procedure. Moreover, the thickness of TCO and BSR layers were never changed and were kept at 0.1 μm and 1 μm respectively. Initially the thickness of buffer layers and absorber layers were kept respectively at 0.02 μm and 2 μm.

The optimum doping concentration of CdTe absorber layer is 2×10^{16} cm^{-3} when ZnS used as buffer layer. But along with CdS layer the most favorable value for of P-type CdTe layer is 2×10^{15} cm^{-3}. Except ITO_ZnS_CZTS solar cell (where the doping concentration value of CZTS is 2×10^{14} cm^{-3}), the best doping concentration value of CZTS absorber layer is 2×10^{15} cm^{-3}.With ZnS as buffer layer the most appropriate doping concentration of CIGS absorber layer is 2×10^{19} cm^{-3}. No specific doping concentration of CIGS absorber layer has been found for CdS buffer layer. The optimum doping concentration values of CIGS absorber layer with CdS as buffer layer are found 2×10^{12} cm^{-3} and 2×10^{16} cm^{-3} respectively for AZO and ITO transparent conductive oxide. As the optimum doping concentration P-type CIGS layer is dissimilar for different cases, it seems that attaining the optimum doping concentration for CIGS absorber layer in the real life fabrication process may be difficult than CdTe and CZTS solar cell.

It has been found in the simulation that except ITO_CdS_CdTe_ZnTe solar cell, by increasing the doping concentration of CdS buffer layers the efficiency of solar cells also increases consequently. Significant increase can be seen when the doping concentration of CdS buffer layers have been increased from 1×10^{17} cm^{-3} and for ITO_CdS_CdTe_ZnTe solar cell 1×10^{17} cm^{-3} produces the best result. It has been observed that by keeping the doping concentration of CZTS layers constant, rising the doping concentrations of ZnS layers from 5×10^{15} cm^{-3} to 5×10^{17} cm^{-3} improves the efficiency of solar cells accordingly. Although ITO_ZnS_CZTS solar cell is an exception of this rule. Where, the optimum doping concentration is same as the reference doping concentration value 5×10^{15} cm^{-3}. Whereas, increment of efficiency of the CdTe solar cell has been found by increasing the doping concentration of ZnS layer from 5×10^{15} cm^{-3} to 5×10^{18} cm^{-3}. But the efficiency of the solar cell increases if the doping concentration of ZnS layer is reduced from 5×10^{15} cm^{-3} to 5×10^{14} cm^{-3} for CIGS solar cell.

The performance of solar cells can be increased by optimizing the thickness of absorber and buffer layers. In this simulation the thickness of CdTe, layers have been changed from 1 to 6 μm. While, the thickness variation of CIGS and CZTS layers have been done from 1 to 4 μm. In all cases of the simulation the efficiency of CZTS solar cells increases in accordance with the increasing thickness of CZTS absorber layers. Here the maximum thickness of CZTS layers are kept at 4 μm. In case of CdTe absorber layer when thickness increases from 2 μm or decrease to 1 μm then efficiency of the CdTe solar cells decreases. Tinedert et al. also found using Silvaco-Atlas simulation software that CdTe thicknesses lower than 2 μm strongly penalize the solar cell efficiency [8]. For CIGS absorber layers, the lower the thickness the higher the efficiency is. Optimum thickness of CIGS absorber layer has been found 1 μm.

CdS buffer layer has been used as the counterpart to Zns buffer layer in this simulation. Both the buffer layers thickness have been varied from 0.01 to 1 μm. For ZnS layer the optimum thickness has been obtained at 0.02 μm (20 nm). Whereas, for CdS layer the optimum thickness has been acquired at 0.01 μm (10 nm). When the thickness of buffer layers increases from 0.01 μm then the efficiency of the solar cells decreases. Nykyruy et al. investigations also tells that the decrease of CdS window layer thickness leads to an increase in the efficiency and 10 nm thickness is the best [9]. Because of decreasing the thickness of CdS layer, it leads directly to the increase in the performance of the absorber layer of solar cells through decreasing the absorption losses that take place in the CdS layer and thus increase in higher short circuit current [55]. In practical situation achieving such low thickness of 0.01 μm (10 nm) can be of some difficulty. Because in the nanometer range there may be some complications due to miniaturization. So far, the CdS layer thickness of 50 nm is the technologically minimal limit for the open evaporation method [55].

It has been observed from the solar cell simulations that, for most of the cases CdS Buffer layer has better efficiency than its counterpart ZnS buffer layer. Although, the best efficiency has been obtained with CZTS solar cell having ZnS as buffer layer. Highest efficiency of 23.67% has been achieved with AZO_ZnS_CZTS solar cell. The Open Circuit Voltage (Voc), Short Circuit Current (Isc), Maximum Power (Pm), Fill factor (FF) and Efficiency are 0.97 V, 27.94 mA/cm^2, 23.67 mW/cm^2, 87.35% and 23.67% respectively. The best efficiency of 23.67% has been achieved by CZTS layer having 4 μm thickness. However,

the efficiency could have been further increased by increasing the CZTS layer thickness. But has not been done so as simulation with CZTS layer with maximum 4 μm thickness has been found in the literature […].If the thickness of CZTS was made 2 μm (which may be more feasible to fabrication and less cost effective than 4 μm thickness) then the best efficiency would not be achieved by AZO_ZnS_CZTS solar cell but by AZO_CdS_CdTe_ZnTe solar cell. Overall AZO_CdS_CdTe_ZnTe solar cell has the second best result with 23.47% efficiency. The Open Circuit Voltage (Voc), Short Circuit Current (Isc), Maximum Power (Pm), Fill factor (FF) and Efficiency of AZO_CdS_CdTe_ZnTe solar cell are 0.93V, 31.20 mA/cm^2, 23.49 mW/cm^2, 80.95% and 23.49% respectively.

Table 4 indicates that, the overall performance of CIGS solar cells are not as good as CdTe or CZTS solar cells. It may be due to the this reason, band gap tuning of CIGS absorber layer has not been done here. As stated earlier, the bandgap of CIGS layer varies from 1.1 to 1.5eV. Here, the bandgap has been kept fixed at 1.13 eV. If the bandgap of CIGS layers are tuned, then the efficiency of CIGS solar cells might be better than CdTe or CZTS solar cells. The maximum efficiency of 22.53% has been attained from AZO_CdS_CIGS_ZnTe solar cell. The Open Circuit Voltage (Voc), Short Circuit Current (Isc), Maximum Power (Pm), Fill factor (FF) and Efficiency AZO_CdS_CIGS_ZnTe solar cell are 0.73V, 43.15 mA/cm^2, 22.53 mW/cm^2, 71.51% and 22.53 % respectively.

In the simulation, efficiency of the solar cells with AZO layers are always found better than solar cells with ITO layers. Result shows that ITO layer overall works well with CZTS solar cells, specifically with ITO_CdS_CZTS solar cell. Where the Open Circuit Voltage (Voc), Short Circuit Current (Isc), Maximum Power (Pm), Fill factor (FF) and Efficiency of ITO_CdS_CZTS solar cell are 0.97 V, 25.16 mA/cm^2, 21.31 mW/cm^2, 87.31% and 21.31% respectively. The I-V Curves of best CdTe, CIGS and CZTS solar cell are shown in Fig. 6.

Table 4
Different Thin Film Solar Cells with their Efficiencies, Voltage and Current

AZO_CdS_CdTe_ZnTe									AZO_CdS_CIGS_ZnTe						
Dc of P-type CdTe (cm^{-3})	Dc of N-type CdS (cm^{-3})	Jsc (mA/cm^2)	Voc (V)	P_m (mW/cm^2)	FF (%)	η (%)	t of CdTe (μm)	t of CdS (μm)	Dc of P-type CIGS (cm^{-3})	Dc of N-type CdS (cm^{-3})	Jsc (mA/cm^2)	Voc (V)	P_m (mW/cm^2)	FF (%)	η (%)
2×10^{16}	1×10^{17}	28.04	0.98	20.21	73.56	20.21	2	0.02	2×10^{16}	1×10^{17}	39.07	0.66	7.58	29.39	7.58
2×10^{16}	1×10^{20}	27.72	0.97	22.27	82.84	22.27	2	0.02	2×10^{12}	1×10^{17}	42.61	0.71	8.89	29.37	8.89
2×10^{15}	1×10^{20}	30.09	0.92	22.40	80.91	22.40	2	0.02	2×10^{12}	1×10^{19}	42.05	0.70	20.95	71.19	20.9
2×10^{15}	1×10^{20}	31.20	0.93	23.49	80.95	23.49	2	0.01	2×10^{12}	1×10^{19}	43.15	0.73	22.53	71.51	22.5
AZO_CdS_CZTS									**AZO_ZnS_CdTe_ZnTe**						
Dc of P-type CZTS (cm^{-3})	Dc of N-type CdS (cm^{-3})	Jsc (mA/cm^2)	Voc (V)	P_m (mW/cm^2)	FF (%)	η (%)	t of CZTS (μm)	t of CdS (μm)	Dc of P-type CdTe (cm^{-3})	Dc of N-type ZnS (cm^{-3})	Jsc (mA/cm^2)	Voc (V)	P_m (mW/cm^2)	FF (%)	η (%)
2×10^{12}	1×10^{17}	27.48	0.75	10.12	49.11	10.12	2	0.02	2×10^{15}	5×10^{15}	31.22	0.93	15.04	51.81	15.0
2×10^{14}	1×10^{17}	27.48	0.89	13.92	56.92	13.92	2	0.02	2×10^{16}	5×10^{15}	28.67	0.98	17.88	63.64	17.8
2×10^{15}	1×10^{18}	27.65	0.97	23.16	86.36	23.16	4	0.01	2×10^{16}	5×10^{18}	29.00	0.98	19.12	67.29	19.1
AZO_ZnS_CIGS_ZnTe									**AZO_ZnS_CZTS**						
Dc of P-type CIGS (cm^{-3})	Dc of N-type ZnS (cm^{-3})	Jsc (mA/cm^2)	Voc (V)	P_m (mW/cm^2)	FF (%)	η (%)	t of CIGS (μm)	t of ZnS (μm)	Dc of P-type CZTS (cm^{-3})	Dc of N-type ZnS (cm^{-3})	Jsc (mA/cm^2)	Voc (V)	P_m (mW/cm^2)	FF (%)	η (%)
2×10^{19}	5×10^{15}	25.77	0.81	17.90	85.75	17.90	2	0.02	2×10^{13}	5×10^{15}	27.97	0.80	18.73	83.69	18.7
2×10^{16}	5×10^{15}	28.39	0.63	14.57	81.45	14.57	2	0.02	2×10^{14}	5×10^{15}	27.97	0.88	21.14	85.90	21.1
2×10^{19}	5×10^{14}	25.77	0.81	17.90	85.75	17.90	2	0.02	2×10^{15}	5×10^{17}	27.89	0.95	22.90	86.44	22.9
2×10^{19}	5×10^{14}	26.35	0.82	18.51	85.65	18.51	1	0.02	2×10^{15}	5×10^{17}	27.94	0.97	23.67	87.35	23.6
ITO_CdS_CdTe_ZnTe									**ITO_ZnS_CdTe_ZnTe**						
Dc of P-type CdTe (cm^{-3})	Dc of N-type CdS (cm^{-3})	Jsc (mA/cm^2)	Voc (V)	P_m (mW/cm^2)	FF (%)	η (%)	t of CdTe (μm)	t of CdS (μm)	Dc of P-type CdTe (cm^{-3})	Dc of N-type ZnS (cm^{-3})	Jsc (mA/cm^2)	Voc (V)	P_m (mW/cm^2)	FF (%)	η (%)
2×10^{12}	1×10^{17}	28.36	0.97	19.92	72.43	19.92	2	0.02	2×10^{15}	5×10^{15}	27.84	0.93	13.74	53.07	13.7
2×10^{16}	1×10^{17}	24.91	0.97	18.27	75.63	18.27	2	0.02	2×10^{16}	5×10^{15}	25.39	0.98	15.79	63.44	15.7
2×10^{15}	1×10^{17}	28.30	0.92	20.53	78.84	20.53	2	0.01	2×10^{16}	5×10^{18}	25.61	0.98	16.75	66.72	16.7
ITO_CdS_CZTS									**ITO_CdS_CIGS_ZnTe**						
Dc of P-type CZTS (cm^{-3})	Dc of N-type CdS (cm^{-3})	Jsc (mA/cm^2)	Voc (V)	P_m (mW/cm^2)	FF (%)	η (%)	t of CZTS (μm)	t of CdS (μm)	Dc of P-type CIGS (cm^{-3})	Dc of N-type CdS (cm^{-3})	Jsc (mA/cm^2)	Voc (V)	P_m (mW/cm^2)	FF (%)	η (%)
2×10^{12}	1×10^{17}	24.52	0.73	14.29	79.83	14.29	2	0.02	2×10^{15}	1×10^{17}	24.44	0.58	10.46	73.78	10.4
2×10^{14}	1×10^{17}	24.52	0.88	18.12	83.97	18.12	2	0.02	2×10^{16}	1×10^{17}	24.06	0.63	11.55	76.20	11.5
2×10^{15}	1×10^{17}	24.45	0.95	19.66	84.64	19.66	2	0.02	2×10^{16}	1×10^{20}	23.40	0.62	11.82	81.45	11.8

AZO_CdS_CdTe_ZnTe									AZO_CdS_CIGS_ZnTe						
2×10^{15}	1×10^{18}	25.16	0.97	21.31	87.31	21.31	4	0.01	2×10^{16}	1×10^{20}	25.34	0.63	13.01	81.51	13.0
ITO_ZnS_CIGS_ZnTe									ITO_ZnS_CZTS						
Dc of P-type CIGS (cm^{-3})	Dc of N-type ZnS (cm^{-3})	Jsc (mA/cm^2)	Voc (V)	P_m (mW/cm^2)	FF (%)	η (%)	t of CIGS (μm)	t of ZnS (μm)	Dc of P-type CZTS (cm^{-3})	Dc of N-type ZnS (cm^{-3})	Jsc (mA/cm^2)	Voc (V)	P_m (mW/cm^2)	FF (%)	η (%)
2×10^{16}	5×10^{15}	25.18	0.62	12.70	81.37	12.70	2	0.02	2×10^{13}	5×10^{15}	25.03	0.80	16.76	83.68	16.7
2×10^{19}	5×10^{15}	22.61	0.81	15.79	86.24	15.79	2	0.02	2×10^{14}	5×10^{15}	25.03	0.88	18.94	85.98	18.9
2×10^{19}	5×10^{14}	23.15	0.81	16.16	86.18	16.16	1	0.02	2×10^{14}	5×10^{15}	25.03	0.90	19.52	86.65	19.5

Footnote

D_c is donor concentration, Jsc is short circuit current density, Voc is open circuit voltage, FF is fill factor, η is efficiency and t is thickness.

5. Conclusion

In this work, simulations have been performed for CdTe, CIGS and CZTS solar cells using WxAMPS software. In addition, all the solar cells have been simulated with different buffer layers and TCO layers such as CdS, ZnS, AZO and ITO. The efficiency of the solar cells have been observed by varying the thickness and doping concentrations of TCO layers, buffer layers, and absorber layers. Moreover, (except CZTS solar cells) the impacts of with and without Zinc telluride (ZnTe) Back-Surface Reflector (BSR) layer has also been investigated. Furthermore, the simulation work is unique in this perspective that, optical parameters (absorption coefficients) values found in the literature have been used for all the layers of CdTe, CIGS and CZTS solar cells. From the simulation, it is observed that, for all the cases of TCOs thickness ranging from 0.1 to 1 μm, the maximum efficiency has been achieved for 0.1 μm. While, the dispute over AZO vs. ITO as TCO is still ongoing and both TCO materials are at present used by the manufacturers, AZO's output outperforms ITO's in this simulation. The results show that (except CZTS solar cell) a thin film solar cell with a ZnTe BSR layer performs better than one without. Solar cell simulations have shown that the CdS buffer layer has a higher efficiency than the ZnS buffer layer in the vast majority of cases. Although, the best efficiency has been obtained with CZTS solar cell having ZnS as buffer layer. The best efficiency of CdTe, CIGS, and CZTS solar cells have been found respectively for AZO_ZnS_CZTS, AZO_CdS_CdTe_ZnTe, and AZO_CdS_CIGS_ZnTe solar cells. The efficiency of these solar cells is 23.67%, 23.47% and 22.53% efficiency respectively. After optimization, all three solar cells shows promising results. Thus, it is hoped that this study will help the novices, scientistis, researchers and manufacturers to understand the behavior of CdTe, CIGS and CZTS thin film solar cells and to fabricate high-efficiency thin film solar cells in the near future.

6. Declarations

Acknowledgments

The authors express their thanks to Prof. Rockett, Dr. Yiming Liu of the University of Illinois at Urbana Champaign, U.S.A. and Prof. Fonash of Pennsylvania State University, U.S.A. for providing the WxAMPS software.

7. References

[1] A. Le Donne, V. Trifiletti and S. Binetti, "New Earth-Abundant Thin Film Solar Cells Based on Chalcogenides", *Frontiers in Chemistry*, vol. 7, 2019. Available: 10.3389/fchem.2019.00297 [Accessed 30 April 2021].

[2] "Solar PV – Analysis - IEA", *IEA*. [Online]. Available: https://www.iea.org/reports/solar-pv. [Accessed: 30- Apr- 2021].

[3] "Thin-Film Solar PV Market | Growth, Trends, and Forecast (2020 - 2025)", *Mordorintelligence.com*. [Online]. Available: https://www.mordorintelligence.com/industry-reports/global-thin-film-solar-collector-market-industry. [Accessed: 30- Apr- 2021].

[4] "Thin Film Solar Cells Market Share Forecast 2024 - Industry Report", *Global Market Insights, Inc.*, 2021. [Online]. Available: https://www.gminsights.com/industry-analysis/thin-film-solar-cells-market. [Accessed: 30- Apr- 2021].

[5] "Solar PV Panels Market Size & Share Report, 2020-2027", *Grandviewresearch.com*. [Online]. Available: https://www.grandviewresearch.com/industry-analysis/solar-panels-market. [Accessed: 30- Apr- 2021].

[6] *Eia.gov*. [Online]. Available: https://www.eia.gov/todayinenergy/detail.php?id=40873. [Accessed: 30- Apr- 2021].

[7] M. Green, E. Dunlop, J. Hohl-Ebinger, M. Yoshita, N. Kopidakis and X. Hao, "Solar cell efficiency tables (version 57)", *Progress in Photovoltaics: Research and Applications*, vol. 29, no. 1, pp. 3-15, 2020. Available: 10.1002/pip.3371 [Accessed 30 April 2021].

[8] I. Tinedert, F. Pezzimenti, M. Megherbi and A. Saadoune, "Design and simulation of a high efficiency CdS/CdTe solar cell", *Optik*, vol. 208, p. 164112, 2020. Available: 10.1016/j.ijleo.2019.164112 [Accessed 1 May 2021].

[9] L. Nykyruy, R. Yavorskyi, Z. Zapukhlyak, G. Wisz and P. Potera, "Evaluation of CdS/CdTe thin film solar cells: SCAPS thickness simulation and analysis of optical properties", *Optical Materials*, vol. 92, pp. 319-329, 2019. Available: 10.1016/j.optmat.2019.04.029 [Accessed 1 May 2021].

[10] D. Parashar, V. Krishna, S. Moger, R. Keshav and M. Mahesha, "Thickness Optimization of ZnO/CdS/CdTe Solar Cell by Numerical Simulation", *Transactions on Electrical and Electronic Materials*, vol. 21, no. 6, pp. 587-593, 2020. Available: 10.1007/s42341-020-00209-9 [Accessed 1 May 2021].

[11] Shoewu, O Anuforonini, G & Duduyemi, O, "Simulation of the Performance of CdTe/CdS/ZnO Multi- Junction Thin Film Solar Cell", *Review of Information Engineering and Applications*, vol. 3, no. 1, pp. 1-10, 2016. Available: 10.18488/journal.79/2016.3.1/79.1.1.10 [Accessed 1 May 2021].

[12] H. Fardi and F. Buny, "Characterization and Modeling of CdS/CdTe Heterojunction Thin-Film Solar Cell for High Efficiency Performance", *International Journal of Photoenergy*, vol. 2013, pp. 1-6, 2013. Available: 10.1155/2013/576952 [Accessed 1 May 2021].

[13] Rihana, S. Ahmed and M. Khalid, "Simulation of CIGS based solar cells with SnO2 window layer using SCAPS-1D", 2019 International Conference on Power Electronics, Control and Automation (ICPECA), 2019. Available: 10.1109/icpeca47973.2019.8975461 [Accessed 2 May 2021].

[14] H. Heriche, Z. Rouabah and N. Bouarissa, "New ultra thin CIGS structure solar cells using SCAPS simulation program", International Journal of Hydrogen Energy, vol. 42, no. 15, pp. 9524-9532, 2017. Available: 10.1016/j.ijhydene.2017.02.099 [Accessed 2 May 2021].

[15] M. Elbar and S. Tobbeche, "Numerical Simulation of CGS/CIGS Single and Tandem Thin-film Solar Cells using the Silvaco-Atlas Software", Energy Procedia, vol. 74, pp. 1220-1227, 2015. Available: 10.1016/j.egypro.2015.07.766 [Accessed 2 May 2021].

[16] B. Farhadi and M. Naseri, "Structural and physical characteristics optimization of a dual junction CGS/CIGS solar cell: A numerical simulation", Optik, vol. 127, no. 21, pp. 10232-10237, 2016. Available: 10.1016/j.ijleo.2016.08.029 [Accessed 2 May 2021].

[17] A. Benmir and M. Aida, "Analytical Modeling and Simulation of CIGS Solar Cells", Energy Procedia, vol. 36, pp. 618-627, 2013. Available: 10.1016/j.egypro.2013.07.071 [Accessed 2 May 2021].

[18] R. Mohottige and S. Kalawila Vithanage, "Numerical simulation of a new device architecture for CIGS-based thin-film solar cells using 1D-SCAPS simulator", Journal of Photochemistry and Photobiology A: Chemistry, vol. 407, p. 113079, 2021. Available: 10.1016/j.jphotochem.2020.113079 [Accessed 2 May 2021].

[19] B. Barman and P. Kalita, "Influence of back surface field layer on enhancing the efficiency of CIGS solar cell", Solar Energy, vol. 216, pp. 329-337, 2021. Available: 10.1016/j.solener.2021.01.032 [Accessed 2 May 2021].

[20] F. Jhuma, M. Shaily and M. Rashid, "Towards high-efficiency CZTS solar cell through buffer layer optimization", Materials for Renewable and Sustainable Energy, vol. 8, no. 1, 2019. Available: 10.1007/s40243-019-0144-1 [Accessed 2 May 2021].

[21] F. Belarbi, W. Rahal, D. Rached, S. benghabrit and M. Adnane, "A comparative study of different buffer layers for CZTS solar cell using Scaps-1D simulation program", Optik, vol. 216, p. 164743, 2020. Available: 10.1016/j.ijleo.2020.164743 [Accessed 2 May 2021].

[22] A. Cherouana and R. Labbani, "Numerical simulation of CZTS solar cell with silicon back surface field", Materials Today: Proceedings, vol. 5, no. 5, pp. 13795-13799, 2018. Available: 10.1016/j.matpr.2018.02.020.

[23] A. Haddout, A. Raidou and M. Fahoume, "A review on the numerical modeling of CdS/CZTS-based solar cells", Applied Physics A, vol. 125, no. 2, 2019. Available: 10.1007/s00339-019-2413-3 [Accessed 2 May 2021].

[24] A. Bouarissa, A. Gueddim, N. Bouarissa and H. Maghraoui-Meherezi, "Modeling of ZnO/MoS2/CZTS photovoltaic solar cell through window, buffer and absorber layers optimization", Materials Science and Engineering: B, vol. 263, p. 114816, 2021. Available: 10.1016/j.mseb.2020.114816 [Accessed 2 May 2021].

[25] K. Sreevidya, N. Abraham and C. sajeev, "Simulation studies of CZTS thin film solar cell using different buffer layers", Materials Today: Proceedings, vol. 43, pp. 3684-3691, 2021. Available: 10.1016/j.matpr.2020.11.405 [Accessed 2 May 2021].

[26] J. Duenow and W. Metzger, "Back-surface recombination, electron reflectors, and paths to 28% efficiency for thin-film photovoltaics: A CdTe case study", Journal of Applied Physics, vol. 125, no. 5, p. 053101, 2019. Available: 10.1063/1.5063799 [Accessed 4 May 2021].

[27] G. Hashmi, M. Imtiaz and S. Rafique, "Towards High Efficiency Solar Cells: Composite Metamaterials", Global Journal of Researches in Engineering: Electrical and Electronics Engineering, vol. 13, no. 10, pp. 11-16, 2013.

[28] "Photovoltaic effect | physics", Encyclopedia Britannica. [Online].

Available: https://www.britannica.com/science/photovoltaic-effect. [Accessed: 20- Apr- 2018].

[29] "Absorber layer as P-type semiconductor material", ResearchGate. [Online]. Available: https://www.researchgate.net/post/In_thin_film_solar_cells_all_absorber_layers_are_p-type_what_is_the_reason. [Accessed: 16- Dec- 2020].

[30] A. Teyou Ngoupo, S. Ouédraogo, F. Zougmoré and J. Ndjaka, "New Architecture towards Ultrathin CdTe Solar Cells for High Conversion Efficiency", International Journal of Photoenergy, vol. 2015, pp. 1-9, 2015. Available: 10.1155/2015/961812 [Accessed 16 December 2020].

[31] "Cadmium Telluride", Energy.gov. [Online]. Available: https://www.energy.gov/eere/solar/cadmium-telluride. [Accessed: 26- Dec- 2020].

[32] Y. Liu, Y. Sun and A. Rockett, "A new simulation software of solar cells—wxAMPS", Solar Energy Materials and Solar Cells, vol. 98, pp. 124-128, 2012. Available: 10.1016/j.solmat.2011.10.010.

[33] S. Fonash et al., "A Manual for AMPS-1D for Windows 95/NT", Pennsylvania State University, 1997. [Accessed 18 December 2020].

[34] Y. Liu, Y. Sun and A. Rockett, "A new simulation software of solar cells—wxAMPS", Solar Energy Materials and Solar Cells, vol. 98, pp. 124-128, 2012. Available: 10.1016/j.solmat.2011.10.010 [Accessed 18 December 2020].

[35] R. Sultana, A. Bahar, M. Asaduzzaman, M. Bhuiyan and K. Ahmed, "Numerical dataset for analyzing the performance of a highly efficient ultrathin film CdTe solar cell", Data in Brief, vol. 12, pp. 336-340, 2017. Available: 10.1016/j.dib.2017.04.015.

[36] S. Sundaram, K. Shanks and H. Upadhyaya, "Thin Film Photovoltaics", A Comprehensive Guide to Solar Energy Systems, pp. 361-370, 2018. Available: 10.1016/b978-0-12-811479-7.00018-x [Accessed 5 May 2021].

[37] M. Asaduzzaman, M. Hasan and A. Bahar, "An investigation into the effects of band gap and doping concentration on Cu(In,Ga)Se2 solar cell efficiency", SpringerPlus, vol. 5, no. 1, 2016. Available: 10.1186/s40064-016-2256-8 [Accessed 5 May 2021].

[38] M. Asaduzzaman, M. Hosen, M. Ali and A. Bahar, "Non-Toxic Buffer Layers in Flexible Cu(In,Ga)Se2Photovoltaic Cell Applications with Optimized Absorber Thickness", International Journal of Photoenergy, vol. 2017, pp. 1-8, 2017. Available: 10.1155/2017/4561208 [Accessed 5 May 2021].

[39] A. Acevedo-Luna, R. Bernal-Correa, J. Montes-Monsalve and A. Morales-Acevedo, "Design of thin film solar cells based on a unified simple analytical model", Journal of Applied Research and Technology, vol. 15, no. 6, pp. 599-608, 2017. Available: 10.1016/j.jart.2017.08.002 [Accessed 5 May 2021].

[40] S. Fatemi Shariat Panahi, A. Abbasi, V. Ghods and M. Amirahmadi, "Analysis and improvement of CIGS solar cell efficiency using multiple absorber substances simultaneously", Journal of Materials Science: Materials in Electronics, vol. 31, no. 14, pp. 11527-11537, 2020. Available: 10.1007/s10854-020-03700-4 [Accessed 5 May 2021].

[41] H. Heriche, Z. Rouabah and L. Selmani, "Thickness Optimization of Various Layers of CZTS Solar Cell", Journal of New Technology and Materials, vol. 4, no. 1, pp. 27-30, 2014. Available: 10.12816/0010293 [Accessed 5 May 2021].

[42] S. Oyedele and B. Aka, "Numerical Simulation of Varied Buffer Layer of Solar Cells Based on Cigs", Modeling and Numerical Simulation of Material Science, vol. 07, no. 03, pp. 33-45, 2017. Available: 10.4236/mnsms.2017.73003 [Accessed 5 May 2021].

[43] R. Treharne, A. Seymour-Pierce, K. Durose, K. Hutchings, S. Roncallo and D. Lane, "Optical Design and Fabrication of Fully Sputtered CdTe/CdS Solar Cells", *Journal of Physics: Conference Series*, vol. 286, p. 012038, 2011. Available: 10.1088/1742-6596/286/1/012038.

[44] K. Sato and S. Adachi, "Optical properties of ZnTe", *Journal of Applied Physics*, vol. 73, no. 2, pp. 926-931, 1993. Available: 10.1063/1.353305.

[45] H. ElAnzeery et al., "Refractive index extraction and thickness optimization of Cu2ZnSnSe4 thin film solar cells", *physica status solidi (a)*, vol. 212, no. 9, pp. 1984-1990, 2015. Available: 10.1002/pssa.201431807.

[46] M. Querry, "Optical constants of minerals and other materials from the millimeter to the ultraviolet, Contractor Report CRDEC-CR-88009", *Apps.dtic.mil*, 1987. [Online]. Available: https://apps.dtic.mil/sti/pdfs/ADA192210.pdf. [Accessed: 06- May- 2021].

[47] S. Sharbati, I. Gharibshahian and A. Orouji, "Designing of AlxGa1-xAs/CIGS tandem solar cell by analytical model", *Solar Energy*, vol. 188, pp. 1-9, 2019. Available: 10.1016/j.solener.2019.05.074 [Accessed 6 May 2021].

[48] S. Collin et al., "Optical Characterizations and Modelling of Semitransparent Perovskite Solar Cells for Tandem Applications", *Eupvsec-proceedings.com*, 2019. [Online]. Available: https://www.eupvsec-proceedings.com/proceedings?paper=48320. [Accessed: 06- May- 2021].

[49] Z. Holman et al., "Infrared light management in high-efficiency silicon heterojunction and rear-passivated solar cells", *Journal of Applied Physics*, vol. 113, no. 1, p. 013107, 2013. Available: 10.1063/1.4772975.

[50] T. König et al., "Electrically Tunable Plasmonic Behavior of Nanocube–Polymer Nanomaterials Induced by a Redox-Active Electrochromic Polymer", ACS Nano, vol. 8, no. 6, pp. 6182-6192, 2014. Available: 10.1021/nn501601e.

[51] F. Abrinaei, M. Shirazi and M. Hosseinnejad, "Investigation of Growth Dynamics of Nanostructured Aluminum Doped Zinc Oxide Thin Films Deposited for the Solar Cell Applications", Journal of Inorganic and Organometallic Polymers and Materials, vol. 26, no. 1, pp. 233-241, 2015. Available: 10.1007/s10904-015-0307-1 [Accessed 7 May 2021].

[52] G. Lee, P. M., W. Park and J. Kim, "Enhanced Optical and Electrical Properties of ITO/Ag/AZO Transparent Conductors for Photoelectric Applications", International Journal of Photoenergy, vol. 2017, pp. 1-9, 2017. Available: 10.1155/2017/8315802 [Accessed 7 May 2021].

[53]"- Front Contact - Mustang Vac", Mustangvac.com. [Online]. Available: https://www.mustangvac.com/Front-Contact. [Accessed: 07- May- 2021].

[54] K. Shin, E. Jang, J. Cho, J. Yoo, J. Park and O. Byungsung, "Study on the fabrication of back surface reflectors in nano-crystalline silicon thin-film solar cells by using random texturing aluminum anodization", Journal of the Korean Physical Society, vol. 67, no. 6, pp. 1033-1039, 2015. Available: 10.3938/jkps.67.1033 [Accessed 7 May 2021].

[55] H. Mohamed, A. Mohamed and H. Ali, "Theoretical study of ZnS/CdS bi-layer for thin-film CdTe solar cell", Materials Research Express, vol. 5, no. 5, p. 056411, 2018. Available: 10.1088/2053-1591/aac5ae [Accessed 8 May 2021].

Figures

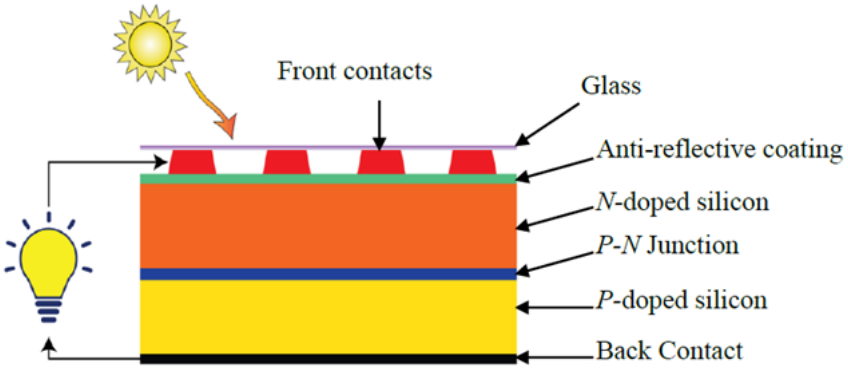

Figure 1

Basic structure of a silicon solar cell.

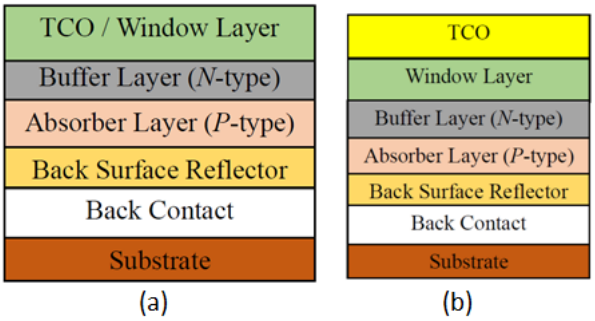

Figure 2

(a): Basic structure of a thin film solar cell where, TCO and window layer being the same. (b): Basic structure of a thin film solar cell where, TCO and window layer being separate layer.

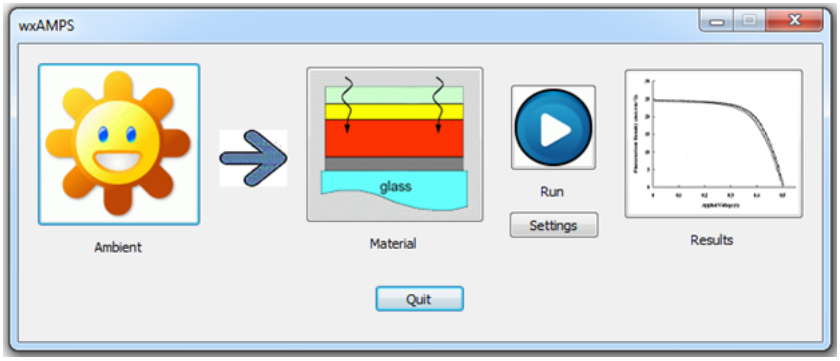

Figure 3

WxAMPS simulation software's the graphical user interface.

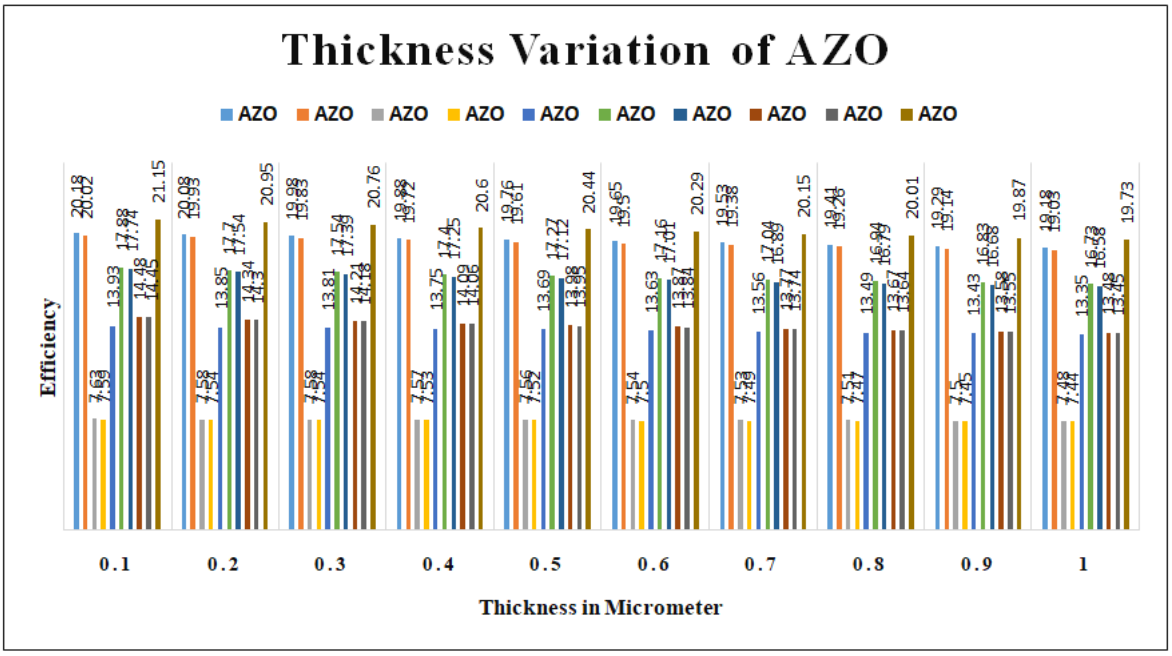

Figure 4

Thickness versus Efficiency Column Chart for AZO.

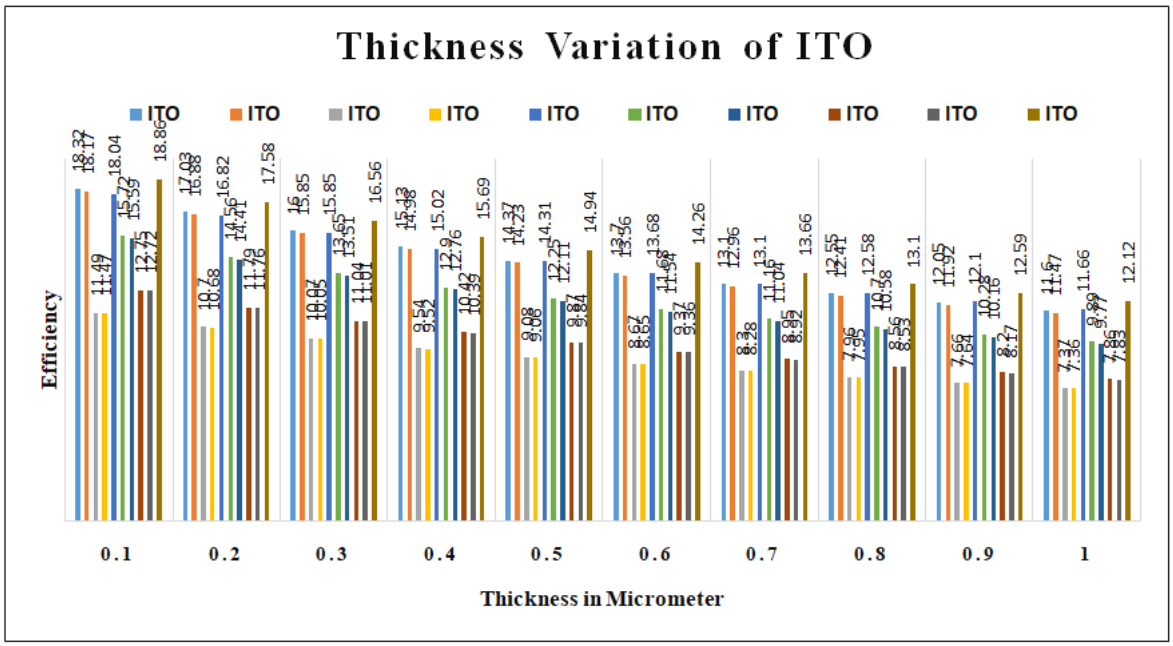

Figure 5

Thickness versus Efficiency Column Chart for ITO.

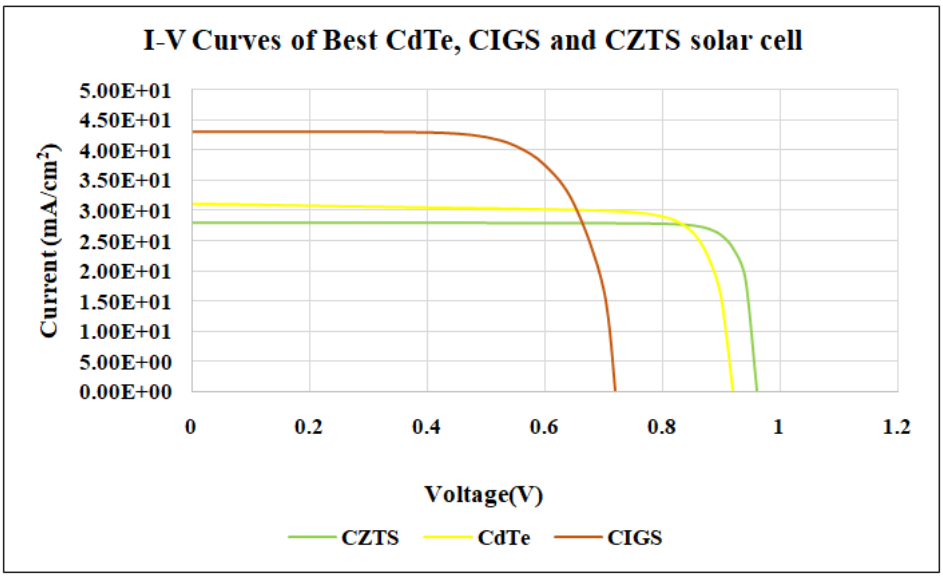

Figure 6

I-V Curves of best CdTe, CIGS and CZTS solar cell